Cyto-biological effects of microRNA-424-5p on human colorectal cancer cells

WEITAO YAN[1,2*], XIA JIANG[1*], GUIQI WANG[1], WEI LI[1], CONGJIE ZHAI[1], SHIHAO CHEN[1], FANGJIAN SHANG[1], ZENGREN ZHAO[1] and WEIFANG YU[3]

[1]Department of General Surgery, Hebei Key Laboratory of Colorectal Cancer Precision Diagnosis and Treatment, The First Hospital of Hebei Medical University, Shijiazhuang, Hebei 050031; [2]Department of Breast Surgery, The First Hospital of Qinhuangdao, Qinhuangdao, Hebei 050000; [3]Department of Endoscopy Center, The First Hospital of Hebei Medical University, Shijiazhuang, Hebei 050031, P.R. China

Received November 28, 2019; Accepted June 19, 2020

DOI: 10.3892/ol.2020.11982

Abstract. MicroRNA (miR)-424-5p is overexpressed in colorectal cancer (CRC); however, its role, clinical significance and underlying molecular mechanism have remained to be fully elucidated. The aim of the present study was to investigate the roles of miR-424-5p in CRC and the underlying mechanisms. It was demonstrated that miR-424-5p is overexpressed in CRC, based on bioinformatics analysis using The Cancer Genome Atlas TCGA and analysis of tissue samples from patients with CRC from The First Hospital of Hebei Medical University, and the expression of miR-424-5p was associated with the depth of invasion and Dukes' staging. In CRC cells, the oncogenic roles of miR-424-5p were also verified by Cell Counting Kit-8, wound healing and Transwell assays. To identify target genes, all transcripts were compared between miR-424-5p mimic-transfected SW480 cells and mimic control cells by transcriptome sequencing. Subsequently, the differentially expressed genes (DEGs) were subjected to Gene Ontology (GO) and Kyoto Encyclopedia of Genes and Genomes (KEGG) analyses. The DEGs were revealed to be significantly enriched in the GO terms 'serine hydrolase activity,' 'serine-type peptidase activity' and 'serine-type endopeptidase activity'. KEGG signaling pathway analysis indicated that the DEGs were significantly enriched in 'endocytosis', 'regulation of actin cytoskeleton', 'Wnt signaling pathway' and 'ubiquitin-mediated proteolysis signaling pathway'. These results suggested that miR-424-5p is a potential target in the treatment of CRC.

Correspondence to: Professor Zengren Zhao, Department of General Surgery, Hebei Key Laboratory of Colorectal Cancer Precision Diagnosis and Treatment, The First Hospital of Hebei Medical University, 89 Donggang Road, Shijiazhuang, Hebei 050031, P.R. China
E-mail: zzr-doctor@163.com

Professor Weifang Yu, Department of Endoscopy Center, The First Hospital of Hebei Medical University, 89 Donggang Road, Shijiazhuang, Hebei 050031, P.R. China
E-mail: ydyynjzx@126.com

*Contributed equally

Key words: microRNA-424-5p, colorectal cancer, proliferation, migration, invasion

Introduction

Colorectal cancer (CRC) is one of the most common malignant diseases worldwide. A previous study showed that are high rates of incidence and disease-associated mortality for CRC (1). The development of effective screening methods to detect cancer is vital as it is necessary for early diagnosis and therapy. To provide novel biological insight and advances in therapy, the molecular mechanisms underlying malignant tumor occurrence and progression are being investigated, with the aim of developing more effective therapies for CRC (2).

MicroRNAs (miRNAs or miRs) are small non-coding RNA molecules, which are endogenous and 18-25 nucleotides in length. The function of miRNAs is to modulate the expression of target mRNAs at a post-transcriptional level and the mechanism of action is by inhibiting mRNA translation or inducing mRNA degradation by binding to a target site (3,4). The target sites may be in the 3' untranslated region (3'-UTR), coding region and the promoter (5,6). It has been reported that miRNAs regulate the expression of >60% of human protein-encoding genes (7). These genes take part in numerous biological processes, including cell proliferation, differentiation, apoptosis, invasion and autophagy (8-10).

miR-424-5p, located at Xq26.3, it is differentially expressed in tumor tissues and normal tissues adjacent to tumors, and it serves different biological functions (11). The expression levels of miR-424-5p are increased in pancreatic (12) and gastric cancer (13); however, the expression levels are decreased in hepatocellular carcinoma, esophageal squamous cell carcinoma and cervical cancer (14-16). The expression and function of miR-424-4p in CRC requires to be reported.

The present study analyzed the miRNA expression profiles using miRNA sequencing data from The Cancer Genome Atlas (TCGA; http://cancergenome.nih.gov/) and determined the cyto-biological effects of miR-424-5p on human CRC cells.

Materials and methods

miRNA array in TCGA for heatmap analysis. Data from TCGA, which is a large-scale cancer genome project that provides genome sequencing data of 33 types of cancer (http://cancergennme.nih.gov/) (17), were analyzed. The data included microRNA sequencing, RNA-sequencing and clinical datasets for various cancer types. In the present study, miRNA array data were obtained from TCGA for heatmap analysis. The sequencing data of miRNAs from 11 adjacent control samples and 619 CRC tissue samples were downloaded from TCGA database and the expression matrix of the miRNAs was aggregated.

Patients and samples. CRC and paired non-tumor adjacent tissue samples, as well as clinicopathological data were collected from patients who underwent radical resection between July 2016 and March 2018 at The First Hospital of Hebei Medical University (Shijiazhuang, China). A total of 59 pairs of CRC and non-tumor adjacent tissues were used for the experiments. The adjacent tissue samples were obtained ≥5 cm from the edge of the tumor. The present study was approved by the Ethics Committee of the First Affiliated Hospital of Hebei Medical University (Shijiazhuang, China; approval nos. 2013106 and 2016004). All patients provided written informed consent for the use of their samples. Following surgical removal, tissues were immediately frozen in liquid nitrogen and stored at -80˚C. The pathological diagnosis of all cancer tissue samples was adenocarcinoma or mucinous carcinoma, all the tissues were pathologically confirmed as cancerous or normal. The clinicopathological data of the patients are presented in Table I.

Cell culture and transfection. The human CRC cell line SW480 was obtained from Professor Xiao-feng Sun (American Type Culture Collection). Detection of mycoplasma free cell was performed using a Mycoplasma Monitoring kit (Vazyme Biotech Co., Ltd.). Cells were cultured in Dulbecco's modified Eagle's medium (DMEM; Gibco; Thermo Fisher Scientific, Inc.) containing 10% fetal bovine serum (FBS; Gibco; Thermo Fisher Scientific, Inc.) and 1% penicillin-streptomycin. All cells were cultured in standard growth medium at 37˚C in a humidified atmosphere with 5% CO_2. miR-424-5p mimic (50 nM; cat. no. HmiR-SN0494), miR-424-5p inhibitor (50 nM; cat. no. HmiR-AN0494-SN-10), mimic control (50 nM; cat. no. CmiR-SN0001-SN) and inhibitor control (50 nM; cat. no. CmiR-AN0001-SN) were purchased from GeneCopoeia, Inc. Lipofectamine 2000 (Invitrogen; Thermo Fisher Scientific, Inc.) was used to perform transfection according to the manufacturer's protocol.

Cell proliferation and colony formation assay. To investigate the role of miR-424-5p in the development of CRC, the cell viability was evaluated using a Cell Counting Kit (CCK)-8 assay (Vazyme Biotech Co., Ltd.), according to the manufacturer's instructions. SW480 cells were transfected with miR-424 mimic, mimic control, miR-424 inhibitor or inhibitor control for 48 h. Logarithmically growing cells were then seeded in 10-cm normal cell culture dishes (3,000 cells/dish) and incubated for 14 days in medium with 10% FBS that was changed every week, and cells were cultured at 37˚C. Subsequently, the colonies were stained with crystal violet (0.5%) for 1 h at room temperature and the number of colonies was counted manually. The colony formation ability was determined in triplicate in tissue culture dishes.

Cell migration and invasion assay. The cell motility capacities were determined using a wound-healing assay and Transwell assay. The wound-healing assay was performed in 6-well culture plates; SW480 cells were seeded in the plate at a density of $50x10^5$ cells/well in culture medium. Following transfection for 48 h, the cells reached 100% confluence and confluent monolayers were scratched with a sterile micro-pipette tip (200 μl), followed by washing with PBS to remove floating cells. The width of the scratch was then measured at 0, 24, 48 and 72 h of incubation in serum-free medium. A total of three independent experiments were performed.

For migration assays, transfected cells ($20x10^5$ per well) in 100 μl serum-free DMEM were plated in the top chamber of a Transwell system (Corning, Inc.), which consisted of 12 wells with an 8.0-μm pore diameter polycarbonate membrane insert. The insert was placed onto a 24-well plate, the bottom chambers of which were filled with 600 μl DMEM with 10% FBS as a chemoattractant. Following 48 h of incubation, the cells remaining on the upper surface of the filter were removed by scraping with a cotton swab, while the cells that had transgressed to the lower surface of the filter were fixed with Diff Quik Fix (mainly methanol) for 2 min, followed by staining with Diff Quik I (eosin) for 2 min and staining with Diff Quik II (mainly methylene blue) for 45 sec. All Diff Quik products were purchased from Zhuhai Beisuo Biology Co, Ltd (BA-4150; www.baso.com.cn). A total of three independent experiments were performed.

For invasion experiments, transfected cells ($20x10^5$ per well) in 200 μl FBS-free DMEM were cultured in the top chamber of a Transwell system that included a Matrigel Invasion Chambers (cat. no. 354480; Corning, Inc.), while the bottom well contained 800 μl medium with FBS. Following incubation for 48 h, cells that had migrated to the lower side of the chamber were stained as specified above. A total of three independent experiments were performed.

Reverse transcription-quantitative PCR (RT-qPCR). Total RNA was extracted from the frozen tissues using TRIzol reagent (Invitrogen; Thermo Fisher Scientific, Inc.), according to the manufacturer's protocol. The concentration and purity of all RNA samples were detected using a NanoDrop ND-2000 spectrophotometer (NanoDrop Technologies; Thermo Fisher Scientific, Inc.).

cDNA synthesis of miRNA was performed using the All-in-One miRNA First-Strand cDNA Synthesis Kit (QP013; GeneCopoeia, Inc.), according to the manufacturer's protocol. qPCR was performed using an All-in-One™ miRNA qPCR kit (QP015; GeneCopoeia, Inc.) with a Roche LightCycler 480 II Real-Time PCR system (Roche Diagnostics) according to the manufacturer's protocol. The sequence-specific primers for mature miR-424-5p (cat. no. HmiRQP0494) and the U6 internal control (cat. no. HmiRQP9001), as well as the Uni-miR qPCR Primer were purchased from GeneCopoeia, Inc. The

Table I. Clinicopathological characteristics of the patients with colorectal cancer (n=59).

Variable	Value, n	miR-424-5p expression	P-value[a]
Age, years			0.4995
<65	36	11.505 (1.895, 105.238)	
≥65	23	7.311 (1.986, 58.081)	
Sex			0.3716
Male	35	12.381 (2.042, 105.420)	
Female	24	6.503 (1.618, 97.400)	
Dukes' stage			0.0159
A,B	32	2.695 (1.518, 43.650)	
C,D	27	32.450 (5.696, 117.800)	
Pathological type			0.0451
Adenocarcinoma	39	12.380 (1.905, 170.100)	
Mucinous carcinoma	20	4.848 (1.641, 26.720)	
Depth of invasion			0.0450
T1,T2	23	3.770 (1.470, 14.670)	
T3,T4	36	33.650 (2.191, 117.400)	
Location			0.5943
Colon	32	7.090 (1.916, 97.400)	
Rectum	27	9.318 (1.905, 117.800)	
Lymph node metastasis			0.6488
Absent	30	7.075 (1.811, 104.900)	
Present	29	9.318 (1.967, 108.600)	
Distant metastasis			0.1495
Absent	49	6.635 (1.854, 95.460)	
Present	10	33.490 (8.706, 116.200)	

[a]According to Mann-Whitney U-test. Values are expressed as the median (interquartile range). miR, microRNA.

relative expression of miR-424-5p was calculated using the $2^{-\Delta\Delta Cq}$ method with normalization to the expression of U6 (18).

A total of 1 μg RNA was reverse-transcribed into cDNA using the PrimeScript RT kit (Takara Bio Inc.) for mRNA detection, at 37˚C for 15 min, and 85˚C for 5 sec. qPCR was subsequently performed using the Power SYBR® Green Master mix (Applied Biosystems; Thermo Fisher Scientific, Inc.), according to the manufacturer's protocol (step 1: 95˚C for 10 min; step 2 for 40 cycles: 95˚C for 15 sec, 60˚C for 1 min). The following primer pairs were used for the qPCR: WNT6, Forward: 5'-CGTAGGGCGGTCACGATG-3' and reverse: 5'-AACTGGAACTGGCACTCTCG-3'; WNT11, forward: 5'-TCTTTGGGGTGGCACTTCTC-3' and reverse: 5'-TGCCGAGTTCACTTGACGAG-3'; DVL1, forward: 5'-CCTCACTAACCAGCTCCGTG-3' and reverse: 5'-ACGTGTGTGTACAGCCAGTC-3'; RAC3, forward: 5'-CCTTCGAGAATGTTCGTGCC-3' and reverse: 5'-TTCACAGAGCCAATCTCCCG-3'; FZD9, forward: 5'-GAACCCCACACACCTCTAGC-3' and reverse: 5'-CTAATGAGCCTCACGGGGTC-3'; SFRP, forward: 5'-GCTGCACATGAAGAATGGCG-3' and reverse: 5'-GTAGTAGAGGGAGCAGGGGT-3'; FZD2, forward: 5'-GCGAAGCCCTCATGAACAAG-3' and reverse: 5'-CTCCGTCCTCGGAGTGGTTC-3' and GAPDH, forward: 5'-ACCCACTCCTCCACCTTTG-3' and reverse: 5'-CTCTTGTGCTCTTGCTGGG-3'. The expression levels were normalized to the internal reference gene GAPDH and quantified using the $2^{-\Delta\Delta Cq}$ method (18).

Transcriptome sequencing and differential expression analysis. To identify small RNAs and the target genes, SW480 colon cancer cells were transfected with miR-424-5p mimic and mimic control, and following transfection for 48 h, the total RNA was extracted for transcriptome sequencing. A total amount of 3 μg RNA per sample was used for the RNA sample preparations. Sequencing libraries were generated using the NEBNext® Ultra™ RNA Library Prep kit for Illumina® (New England Biolabs) following the manufacturer's protocol and index codes were added to assign sequences to each sample. Library quality was assessed on the Agilent Bioanalyzer 2100 system (Agilent Technologies, Inc.). The clustering of the index-coded samples was performed on a cBot Cluster Generation system using the TruSeq PE Cluster kit v3-cBot-HS (Illumia, Inc.) according to the manufacturer's protocol. Following cluster generation, the library preparations were sequenced on an Illumina Hiseq platform (Illumina, Inc.).

Raw data (raw reads) in fastq format were first processed through in-house perl scripts. Reference genome and gene

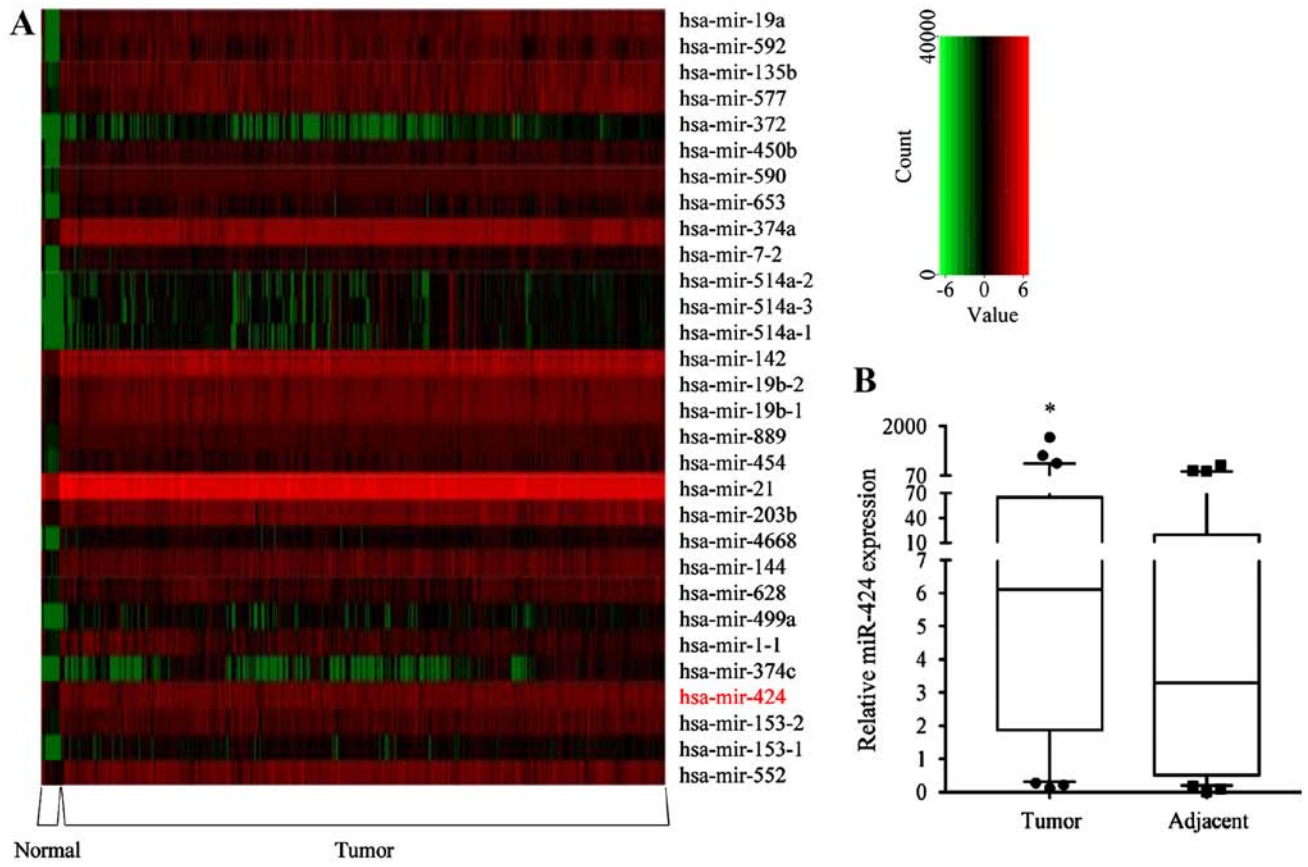

Figure 1. Expression of miR-424-5p is upregulated in human CRC tissues. (A) Heat-map analysis of the top 30 upregulated miRNAs in 619 CRC and 11 normal colorectal tissues from The Cancer Genome Atlas database. The green/black/red color indicates low/medium/high miRNA expression. (B) miR-424-5p expression was determined in 59 CRC tissues (median=6.12, P25=1.87, P75=65.12) and adjacent normal tissues (median=3.29, P25=0.51, P75=19.84) by RT-qPCR analysis. The inter-quartile ranges were shown in the box diagram. *P<0.05 *vs*. adjacent normal tissues, according to the Mann-Whitney U-test. miRNA/miR, microRNA; CRC, colorectal cancer; hsa, *Homo sapiens*; P25, 25% percentile; P75, 75% percentile.

model annotation files were downloaded from the genome website directly. An index of the reference genome was built using Hisat2 v2.0.5 and the Fragments Per Kilobase of transcript per Million mapped reads (FPKM) of each gene were calculated based on the length of the gene and reads count mapped to this gene. The FPKM results were uploaded to Baidu (https://pan.baidu.com/s/1PxiK87dIbhfgZUL2y9nqZg) (extraction code, djau). Differential expression analysis of miR-424-5p mimic/mimic control was performed using the DESeq2 package of R (1.16.1). The resulting P-values were adjusted using the Benjamini and Hochberg approach for controlling the false discovery rate. DEGs were screened from three independent transcriptome sequencing by DESeq2 and genes with an adjusted P<0.05 were considered as DEGs.

Subsequently, disease oncology analysis using the Database for Annotation, Visualization and Integrated Discovery (DAVID, https://david.ncifcrf.gov/) and Kyoto Encyclopedia of Genes and Genomes Orthology Based Annotation System (http://kobas.cbi.pku.edu.cn/index.php), gene ontology (GO) enrichment and Kyoto Encyclopedia of Genes and Genomes (KEGG) pathway analyses of the DEGs were performed using the clusterProfiler package of R.

Statistical analysis. For continuous variables, values are expressed as the median ± standard deviation or the median and 25th and 75th percentiles (interquartile range). All experiments were performed in triplicates. Differences between groups were analyzed using the Mann-Whitney U-test, two-way analysis of variance and correction for multiple comparisons using the Sidak statistical hypothesis test or an unpaired Student's t-test. P<0.05 was considered to indicate a statistically significant difference. SPSS v21.0 (IBM, Corp.) and GraphPad Prism v7.0 (GraphPad Software, Inc.) were used for statistical analysis.

Results

miR-424-5p is upregulated in human CRC tissues. Heatmap analysis of the miRNA expression profiles of 619 CRC and 11 normal colorectal tissues was first performed using the TCGA database. From the series matrix files, 276 DEGs were identified, among which 180 were upregulated and 96 were downregulated (Table SI). The top 30 upregulated miRNAs are presented in a heatmap in Fig. 1A. To further confirm these results, the expression of miR-424-5p in 59 pairs of CRC tissue and corresponding non-tumor colorectal tissue samples was analyzed. The expression of miR-424-5p in the CRC tissues was significantly higher compared with that in the corresponding non-tumor colorectal tissues (P=0.0056; Fig. 1B). The clinicopathological characteristics [age (median=62, 25% percentile (P25)=50.5, P75=72.5); sex (male:female=35:24); Dukes' stage (A,B:C,D=32:27); pathological

Table II. Top 20 upregulated protein-coding differentially expressed genes (miR-424-5p mimic/mimic control, P<0.05).

Gene name	Log_2 (fold-change)	Chromosome	Gene description
SLC10A5	6.529	8	Solute carrier family 10 member 5
C11orf42	6.404	11	Chromosome 11 open reading frame 42
FGL2	6.404	7	Fibrinogen-like 2
B3GAT2	6.269	6	Beta-13-glucuronyltransferase 2
PSG9	6.119	19	Pregnancy-specific beta-1-glycoprotein 9
PKD2L2	5.951	5	Polycystic kidney disease 2-like 2
GCKR	5.951	2	Glucokinase (hexokinase 4) regulator
VWA5A	5.951	11	Von Willebrand factor A domain containing 5A
FRRS1	5.951	1	Ferric-chelate reductase 1
SENP3-EIF4A1	5.951	17	SENP3-EIF4A1 readthrough (NMD candidate)
GREB1L	5.762	18	Growth regulation by estrogen in breast cancer-like
COL23A1	5.762	5	Collagen type XXIII α 1
MRAP	5.762	21	Melanocortin 2 receptor accessory protein
SLC22A9	5.762	11	Solute carrier family 22 (organic anion transporter) member 9
CYP26C1	5.762	10	Cytochrome P450 family 26 subfamily C member 1
SLC46A2	5.762	9	Solute carrier family 46 member 2
RP11-166B2.1	5.762	16	Putative NPIP-like protein LOC729978
GPR182	5.544	12	G protein-coupled receptor 182
PCDHGB5	5.544	5	Protocadherin gamma subfamily B 5
TAL1	5.544	1	T cell acute lymphocytic leukemia 1

Table III. Top 20 downregulated protein-coding differentially expressed genes (miR-424-5p mimic/mimic control, P<0.05).

Gene name	Log_2 (fold-change)	Chromosome	Gene description
CGB5	-6.41484	19	Chorionic gonadotropin beta polypeptide 5
FAM209A	-6.26472	20	Family with sequence similarity 209 member A
ABI3	-6.09713	17	ABI family member 3
SLC6A4	-5.9075	17	Solute carrier family 6 member 4
NANOS2	-5.9075	19	Nanos homolog 2 (Drosophila)
AGXT	-5.9075	2	Alanine-glyoxylate aminotransferase
CLEC17A	-5.9075	19	C-type lectin domain family 17 member A
IL1R2	-5.68911	2	Interleukin 1 receptor type II
SPATA3	-5.68911	2	Spermatogenesis associated 3
REG3A	-5.68911	2	Regenerating family member 3 α
PCED1B	-3.98055	12	PC-esterase domain containing 1B
OMP	-3.78942	11	Olfactory marker protein
TPO	-3.68344	2	Thyroid peroxidase
ERN2	-3.30883	16	Endoplasmic reticulum to nucleus signaling 2
BEND6	-3.30883	6	BEN domain containing 6
ADGRD1	-3.15871	12	Adhesion G protein-coupled receptor D1
GSTM3	-3.06686	1	Glutathione S-transferase mu 3 (brain)
ADGRE1	-3.06686	19	Adhesion G protein-coupled receptor E1
USHBP1	-2.97446	19	Usher syndrome 1C binding protein 1
CCL3	-2.76975	17	Chemokine (C-C motif) ligand 3

type (adenocarcinoma: Mucinous carcinoma=39:20); depth of invasion (T1,T2:T3,T4=23:36); location (colon:rectum=32:27); lymph node metastasis (absent:present=30:29); distant metastasis (absent:present=49:10)] of the patients are presented in Table I. In summary, the results revealed that mR-424-5p is upregulated in CRC tissues.

Table IV. Expression of genes of the Wnt signaling pathway.

Gene name	Fold-change	P-value	Gene description
WNT6	0.2845772	0.00002	Wnt family member 6
WNT11	0.43327208	0.00421	Wnt family member 11
DVL1	0.45380582	0.00614	Dishevelled segment polarity protein 1
RAC3	0.45782965	0.00737	Rac family small GTPase 3
FZD9	0.46584114	0.00921	Frizzled class receptor 9
SFRP5	0.47657406	0.01022	Secreted frizzled-related protein 5
FZD2	0.48708141	0.01351	Frizzled class receptor 2

Fold change: miR-424-5p mimic/mimic control.

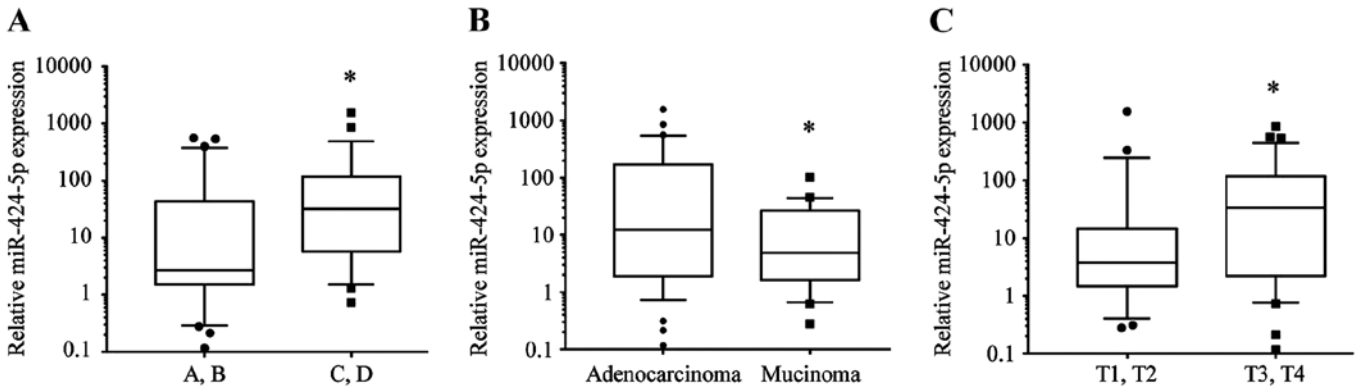

Figure 2. Expression of miR-424-5p is associated with the differentiation and pathological type of CRC. (A) miR-424-5p expression in CRC tissues by Dukes' staging (C,D vs. A,B). (B) miR-424-5p expression in mucinous carcinoma vs. adenocarcinoma. (C) miR-424-5p expression in CRC tissues by infiltration depth (T stage; T3, T4 vs. T1,T2). *P<0.05 according to the Mann-Whitney U-test. miR, microRNA.

miR-424-5p expression is associated with Dukes' stage, depth of invasion and pathological type of CRC. The expression levels of miR-424-5p in CRC tissues were significantly increased in Dukes' stage C.D compared with those in Dukes' stage A.B [median (interquartile range), 32.45 (5.696-117.8) vs. 2.695 (1.518-43.65); P=0.0159; Fig. 2A]. The expression of miR-424-5p in CRC tissues was also increased in adenocarcinoma compared with mucinous carcinoma [12.38 (1.905-170.1) vs. 4.848 (1.641-26.72); P=0.0451; Fig. 2B]. Regarding infiltration depth, the expression levels of miR-424-5p in CRC tissues were upregulated in T3.T4 stage [33.65 (2.191-117.4)] compared with T1.T2 stage [3.77 (1.47-14.67); P=0.0450; Fig. 2C].

Overexpression of miR-424-5p promotes and suppression of miR-424-5p inhibits CRC cell proliferation. To investigate the role of miR-424-5p in the development of CRC, the cell viability was evaluated using a Cell Counting Kit (CCK)-8 assay. The SW480 cells were successfully transfected with miR-424-5p mimic (8.35±0.086) or mimic control (1±0.015), and miR-424-5p inhibitor (0.083±0.009) or inhibitor control (1±0.015; Fig. 3A and B). Following transfection for 24 h, a CCK-8 assay was performed and miR-424-5p expression was measured. The expression of miR-424-5p and cell viability was increased following transfection of miR-424-5p mimic as compared that in the mimic control-transfected SW480 cells at 24, 48, 72 and 96 h (Fig. 3C). Following transfection with miR-424-5p inhibitor, the expression of miR-424-5p and the viability of SW480 cells was significantly decreased as compared with that in the inhibitor control-transfected group at 48, 72 and 96 h (Fig. 3D). A colony formation assay was also performed with SW480 cells transfected with miR-424-5p mimic or mimic control and miR-424-5p inhibitor or inhibitor control. Colony formation by SW480 cells transfected with miR-424-5p mimic was significantly increased compared with that in the mimic control group (Fig. 3E). In the miR-424-5p inhibitor-transfected SW480 group, the colony formation was significantly decreased as compared with that in the inhibitor control group (Fig. 3F). These results indicated that the miR-424-5p expression is positively associated with CRC cell proliferation.

Overexpression of miR-424-5p promotes and suppression of miR-424-5p inhibits the migration and invasion of CRC cells. SW480 cells were transfected with miR-424-5p mimic or mimic control and inhibitor or inhibitor control for 48 h and then subjected to a wound-healing assay. The results revealed that miR-424-5p overexpression promoted CRC cell migration, while silencing of miR-424-5p markedly inhibited CRC cell migration (P<0.05; Fig. 4A and B). Subsequently, Transwell assays were used to examine the effects of miR-424-5p on SW480 cell migration and invasion.

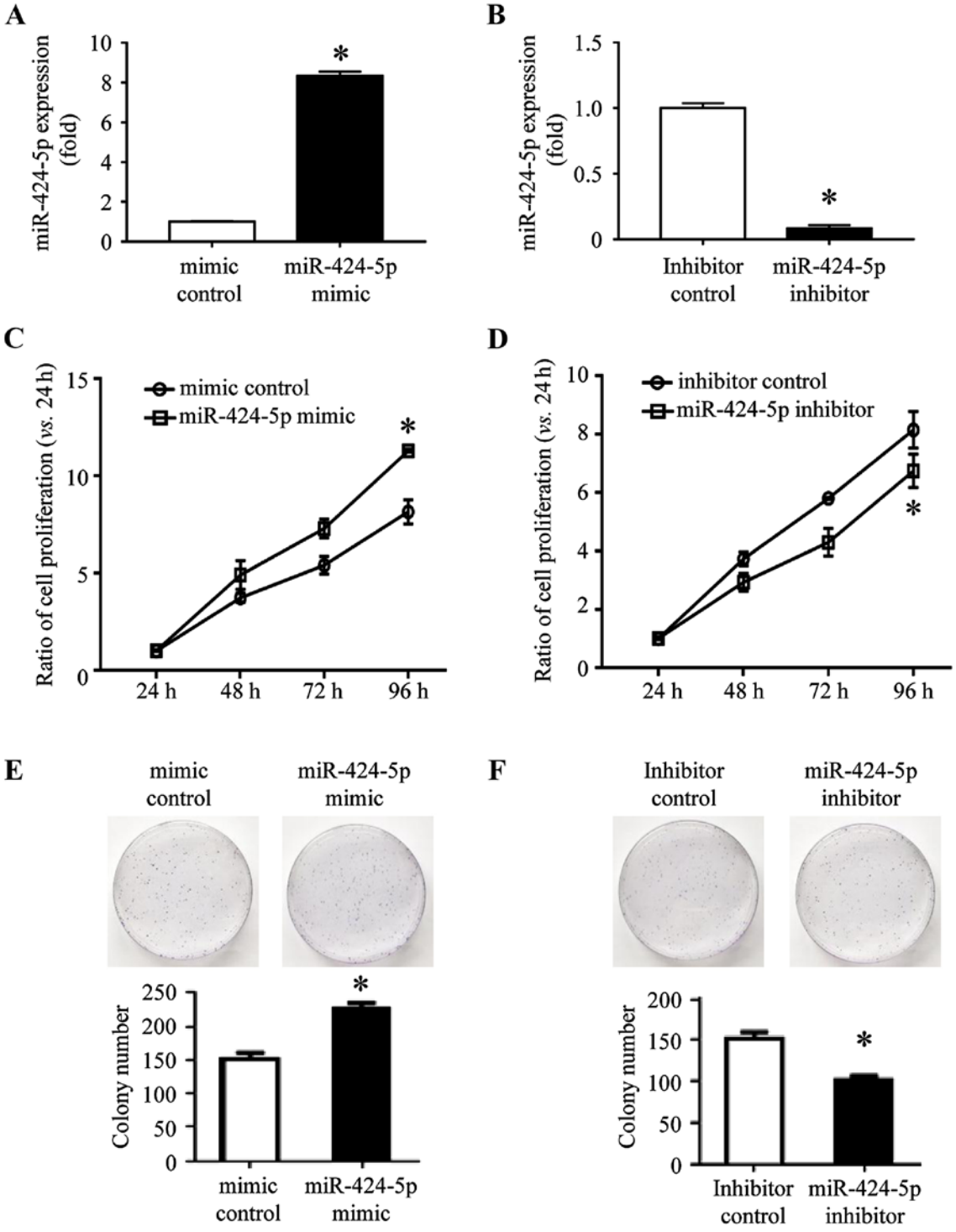

Figure 3. Effects of miR-424-5p on the proliferation of colorectal cancer cells. (A and B) The relative expression levels of miR-424-5p were detected by PCR in SW480 cells transfected with (A) miR-424-5p mimic or mimic control and (B) miR-424-5p inhibitor or inhibitor control. (C and D) Viability of SW480 cells transfected with (C) miR-424-5p mimic or mimic control and (D) miR-424-5p inhibitor or inhibitor control. (E and F) Colony formation ability of SW480 cells transfected with (E) miR-424-5p mimic or mimic control and (F) miR-424-5p inhibitor or inhibitor control. The significance of the difference between the two groups was determined by Student's t-test in A, B, E and F and by two-way analysis of variance in C and D. *P<0.05 vs. control. miR, microRNA.

Overexpression of miR-424-5p significantly promoted, while silencing of miR-424-5p significantly inhibited the migration of CRC cells (P<0.05; Fig. 4C and D). Blue staining represents migrating/invading cells. As presented in Fig. 4E, SW480 cells transfected with miR-424-5p mimic exhibited a significantly higher invasive capacity. However, those transfected with miR-424-5p inhibitor had a significantly lower invasive capacity compared with those transfected with the control (Fig. 4F). Therefore, miR-424-5p was indicated to have a stimulatory effect on the migration and invasion of CRC cells.

Identification and functional characterization of DEGs from the transcriptome sequencing of SW480 cells transfected with miR-424-5p mimic and control. Transcriptome sequencing

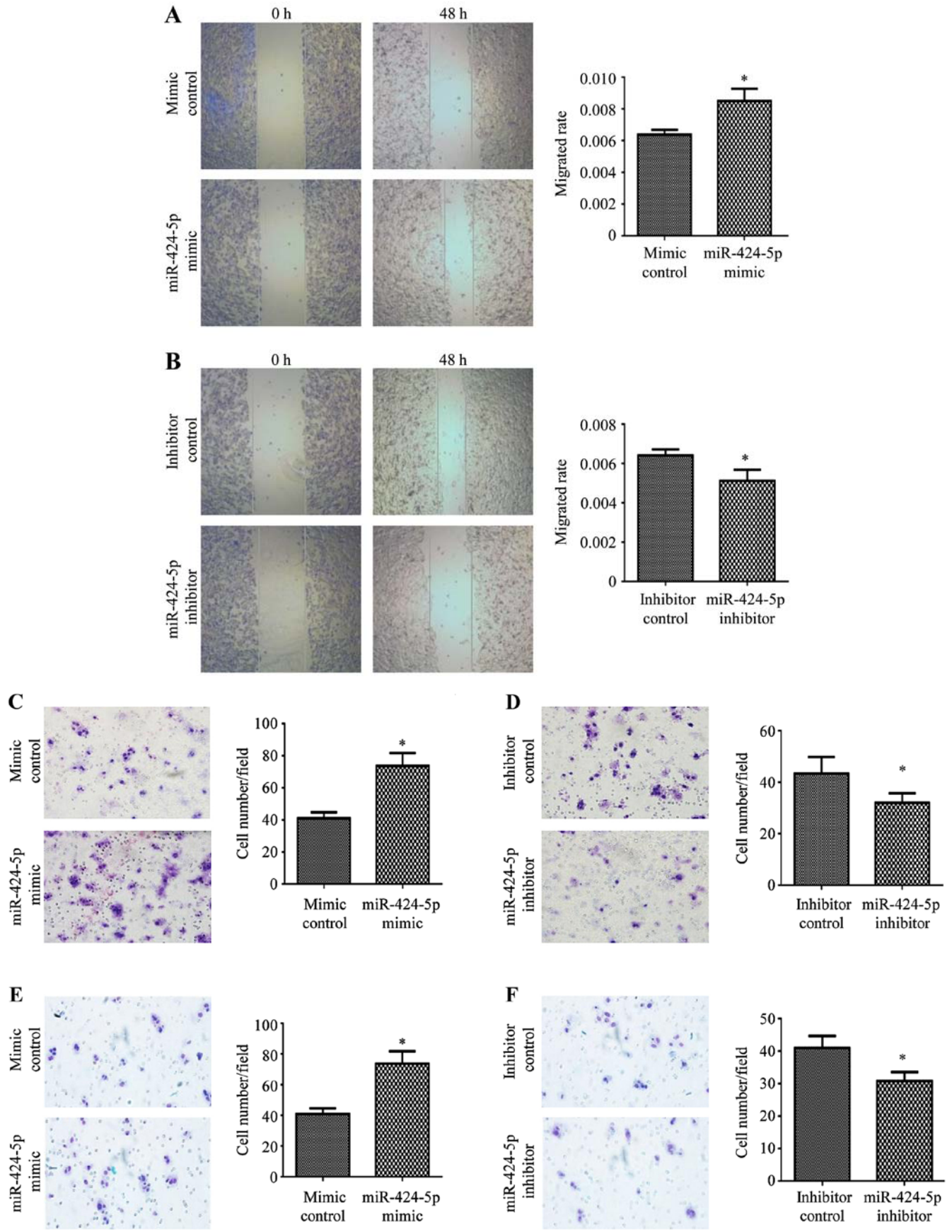

Figure 4. Effects of miR-424-5p on the migration and invasive capability of colorectal cancer cells at 20x magnification. (A and B) Cell migration (scratch wound assay) was determined in SW480 cells transfected with (A) miR-424-5p mimic and mimic control or (B) miR-424-5p inhibitor and inhibitor control. (C and D) Cell migration was determined in SW480 cells transfected with (C) miR-424-5p mimic and mimic control or (D) miR-424-5p inhibitor and inhibitor control. (E and F) Cell invasion capability was determined in SW480 cells transfected with (E) miR-424-5p mimic and mimic control or (F) miR-424-5p inhibitor and inhibitor control. Values are expressed as the mean ± standard deviation of three independent experiments. $^{*}P<0.05$ vs. control. miR, microRNA.

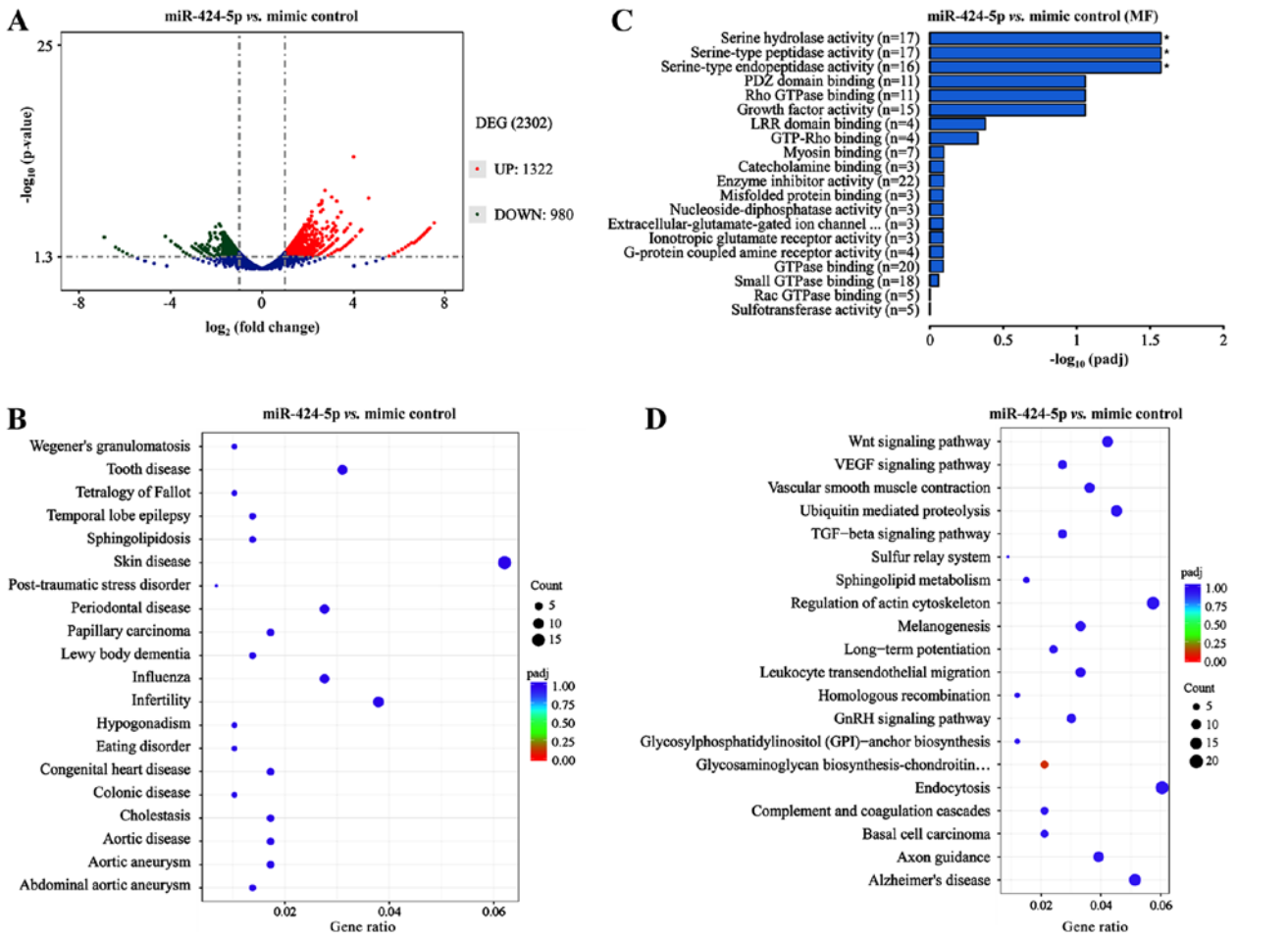

Figure 5. Identification and functional characterization of DEGs from the transcriptome sequencing in the SW480 cells transfected with miR-424-5p mimic and mimic control. (A) Volcano plot of the DEGs between the miR-424-5p mimic- and mimic control-transfected SW480 cells from transcriptome sequencing, including 1,322 upregulated genes (red dots, fold change >2 and P<0.05) and 980 downregulated genes (green dots, fold change ≤2 and P<0.05). (B) Gene ontology analyses revealed that most of the DEGs were significantly enriched in serine hydrolase activity, serine-type peptidase and endopeptidase activity. (C) Disease ontology analysis of the DEGs. The DEGs were enriched in different diseases, including skin disease, infertility and colonic disease. The size of dots indicates the counts of DEGs. (D) Signaling pathway analyses using the Kyoto Encyclopedia of Genes and Genomes indicated that DEGs were enriched in signal transduction MAPK signaling pathway. The size of the dots indicates the counts of DEGs. miR, microRNA; DEG, differentially expressed gene; VEGF, vascular endothelial growth factor; TGF, transforming growth factor.

revealed DEGs between SW480 cells transfected with miR-424-5p mimic and those transfected with the control. These DEGs comprised 1,322 upregulated genes (Table SII) and 980 downregulated genes (Table SIII), including protein-coding genes and non-coding genes (Fig. 5A). The top 20 upregulated protein-coding genes are presented in Table II and the top 20 downregulated protein-coding genes are presented in Table III. GO analyses revealed that the majority of the DEGs were significantly enriched in 'serine hydrolase activity', 'serine-type peptidase' and 'endopeptidase activity' (Fig. 5B). Disease ontology functional enrichment analysis of these DEGs revealed that they were accumulated in different diseases, including skin disease, infertility and colonic diseases (Fig. 5C). Signaling pathway analysis indicated that the DEGs were enriched in the 'Wnt signaling pathway' (Fig. 5D).

Nuclear factor of activated T cells 5, Wnt family member 6 (WNT6), adenomatous polyposis coli, nuclear factor of activated T cells 3, low-density lipoprotein receptor-related protein 6, WNT2B, WNT11, dishevelled segment polarity protein 1 (DVL1), Rac family small GTPase 3 (RAC3), frizzled class receptor 9 (FZD9), secreted frizzled-related protein 5 (SFRP5), frizzled class receptor 2 (FZD2), Rho-associated coiled-coil containing protein kinase 1 (ROCK1) and ROCK2 were enriched in the Wnt signaling pathway; therefore, the expression of these genes was analyzed by RT-qPCR. The expression levels of WNT6, WNT11, DVL1, RAC3, FZD9, SFRP5 and FZD2 were downregulated in miR-424-5p mimic-transfected cells compared with the control cells (Table IV).

Discussion

The expression of miR-424-5p has been reported to be dysregulated in human cancer and may either be up- or down-regulated in tumor tissues depending on the tumor type (19). miR-424-5p was observed to be upregulated in certain types of cancer, including esophageal squamous cell carcinoma (15), gastric cancer (13), pancreatic cancer (12) and tongue squamous cell carcinoma (20), while it was downregulated in others, including epithelial ovarian cancer (11), endometrial carcinoma (21), cervical cancer (22), lung cancer (23),

chronic myeloid leukemia (24), hepatocellular carcinoma (25) and bladder cancer (26). The present study indicated that miR-424-5p was increased in CRC tissues and its association with clinicopathological data were determined. The expression of miR-424-5p was higher in advanced Dukes' stages of CRC (compared with less advanced stages of CRC), deeper invasion depth of tumors (compared with T1&T2 invasion depth of CRC) and adenocarcinoma (compared with mucinous carcinoma). miR-424-5p expression was previously reported to be associated with muscle invasion, high pathological grade, lymph node involvement and distant metastasis in bladder cancer (26). Various studies have reported that the abnormal expression of miR-424-5p is associated with different clinicopathological characteristics in different tumor types. All of these studies suggested that miR-424-5p has an important role in tumor progression.

A large number of studies have indicated that the same miRNA may serve different biological roles in different types of cancer cell by acting as either an oncogene or tumor suppressor. miR-424-5p has been demonstrated to serve as a tumor suppressor in most types of human cancer, including hepatocellular carcinoma (27,28). miR-424-5p has been reported to suppress tumor cell proliferation, migration and invasion through downregulating the expression of c-Myb, catenin beta interacting protein 1 (ICAT) and Akt3. miR-424-5p may function as a tumor suppressor in endometrial carcinoma cells by targeting E2F transcription factor (E2F)7 (21). Similarly, miR-424-5p acts as an oncogene by targeting various genes in cervical cancer (16,29) and breast cancer (19). miR-424-5p has been reported to be aberrantly expressed in several cancer types and to act as a tumor suppressor when downregulated in these cancer types. However, miR-424-5p promotes cell proliferation by targeting Smad3 via the transforming growth factor-β signaling pathway in gastric cancer (13). Various studies have indicated that RNA exhibits different expression and biological functions in different tumor tissue types. The present study demonstrated that miR-424-5p promotes the migration and invasion of the SW480 CRC cell line.

It is understood that miRNA leads to the alteration of mRNA by binding to the 3'-UTR of the gene, leading to the regulation of posttranscriptional gene expression by inhibiting the translation or degradation of mRNA. However, the exact mechanisms, including all of the target genes and targeting interactions, of how miRNAs regulate their target genes remain to be fully elucidated (30). miR-424-5p were also able to supress thousands of target genes expression, including the famous cancer related genes c-Myb, ICAT, Akt3 and E2F3 etc., downregulating of those genes could suppress hepatocellular carcinoma cell proliferation, migration and invasion (19). miRNAs are involved in a number of other oncogenic or carcinogenic networks, which leads to the regulation of several mRNAs. For instance, RAS-responsive element-binding protein (RREB1) and mutant KRAS repress miR-143-5p and the miR-145-5p promoter, and KRAS and RREB1 are targets of miR-145, revealing a feedback mechanism that increases the effect of RAS signaling (31). By performing a sequencing analysis and bioinformatics analysis of the results, the present study demonstrated that miR-424-5p regulates multiple genes. These genes are enriched in different signaling pathways and located in different cell types. Signaling pathway analysis indicated that the DEGs were enriched in 'endocytosis', 'regulation of actin cytoskeleton' and 'Wnt signaling pathway'.

Of note, the present study had certain limitations. For instance, only real-time PCR was used to detect the expression of miR-424-5p and no *in situ* hybridization (ISH) was employed. ISH is a complex technique and its advantage is that paraffin sections may be used. This technology is frequently used when paraffin sections are available (32). When total RNA is extracted from fresh tissue, PCR is more convenient than that ISH to examine the expression of miRNA. However, the intracellular position of miR-424-5p expression cannot be indicated using RT-qPCR.

In conclusion, the present study demonstrated that miR-424-5p, as a key candidate miRNA, was involved in the development of CRC. In addition, miR-424-5p regulated gene expression profiles and pathways of CRC, including the *WNT6, WNT11, DVL1, RAC3, FZD9, SFRP5* and *FZD2* genes. It was also demonstrated to a certain extent that the occurrence and development of tumors is the result of the common action of multiple genes. These candidate genes and pathways may be novel therapeutic targets and biomarkers for CRC.

Acknowledgements

The authors would like to thank Professor Xiao-feng Sun (Division of Oncology, Department of Clinical and Experimental Medicine, Faculty of Health Sciences, Linköping University, Linköping, Sweden) for providing materials.

Funding

This study was supported by the National Natural Science Foundation of China (grant no. 81572758), International Science and Technology Cooperation Program of Hebei (grant nos. 2019YX006A and YZ201802), Natural Science Foundation of Hebei (grant no. H2017206286), Foundation for Distinguished Young Talents in Higher Education of Hebei (grant no. BJ2018042) and The Project of Hebei Province Science and Technology Plan from Hebei province (grant nos. zh2018002, LNB201911, 18077741D, XH201701 and 201805A049).

Availability of data and materials

miRNA array data are available from The Cancer Genome Atlas repository (http://cancergennme.nih.gov/). The datasets used and/or analyzed during the current study are available from the corresponding author on reasonable request.

Authors' contributions

XJ, WFY and ZZ conceived and designed the experiments. WTY, GW, WL, WFY, CZ and SC performed the experiments. WTY, FS and WL collected and analyzed the data. WTY and XJ interpreted the results and wrote the manuscript. All authors read and approved the manuscript and agree to be accountable for all aspects of the research and to guarantee for the accuracy and integrity of any part of the work.

Ethics approval and consent to participate

This study was performed in accordance with standard guidelines and was approved by the Ethics Committee of The First Hospital of Hebei Medical University (Shijiazhuang, China; approval nos. 2013106 and 2016004). All patients provided written informed consent prior to the study.

Patient consent for publication

Not applicable.

Competing interests

The authors declare that they have no competing interests.

References

1. Cao L, Liu Y, Wang D, Huang L, Li F, Liu J, Zhang C, Shen Z, Gao Q, Yuan W and Zhang Y: MiR-760 suppresses human colorectal cancer growth by targeting BATF3/AP-1/cyclinD1 signaling. J Exp Clin Cancer Res 37: 83, 2018.
2. Huang Q and Ma Q: MicroRNA-106a inhibits cell proliferation and induces apoptosis in colorectal cancer cells. Oncol Lett 15: 8941-8944, 2018.
3. Gu S, Jin L, Zhang F, Sarnow P and Kay MA: Biological basis for restriction of microRNA targets to the 3' untranslated region in mammalian mRNAs. Nat Struct Mol Biol 16: 144-150, 2009.
4. Lu J, Getz G, Miska EA, Alvarez-Saavedra E, Lamb J, Peck D, Sweet-Cordero A, Ebert BL, Mak RH, Ferrando AA, *et al*: MicroRNA expression profiles classify human cancers. Nature 435: 834-838, 2005.
5. Ye JJ and Cao J: MicroRNAs in colorectal cancer as markers and targets: Recent advances. World J Gastroenterol 20: 4288-4299, 2014.
6. Fayyad-Kazan H, Bitar N, Najar M, Lewalle P, Fayyad-Kazan M, Badran R, Hamade E, Daher A, Hussein N, ElDirani R, *et al*: Circulating miR-150 and miR-342 in plasma are novel potential biomarkers for acute myeloid leukemia. J Transl Med 11: 31, 2013.
7. Friedman RC, Farh KK, Burge CB and Bartel DP: Most mammalian mRNAs are conserved targets of microRNAs. Genome Res 19: 92-105, 2009.
8. Wang B, Yin M, Cheng C, Jiang H, Jiang K, Shen Z, Ye Y and Wang S: Decreased expression of miR4903p in colorectal cancer predicts poor prognosis and promotes cell proliferation and invasion by targeting RAB14. Int J Oncol 53: 1247-1256, 2018.
9. Kassambara A, Jourdan M, Bruyer A, Robert N, Pantesco V, Elemento O, Klein B and Moreaux J: Global miRNA expression analysis identifies novel key regulators of plasma cell differentiation and malignant plasma cell. Nucleic Acids Res 45: 5639-5652, 2017.
10. Gozuacik D, Akkoc Y, Ozturk DG and Kocak M: Autophagy-regulating microRNAs and Cancer. Front Oncol 7: 65, 2017.
11. Liu J, Gu Z, Tang Y, Hao J, Zhang C and Yang X: Tumour-suppressive microRNA-424-5p directly targets CCNE1 as potential prognostic markers in epithelial ovarian cancer. Cell Cycle 17: 309-318, 2018.
12. Wu K, Hu G, He X, Zhou P, Li J, He B and Sun W: MicroRNA-424-5p suppresses the expression of SOCS6 in pancreatic cancer. Pathol Oncol Res 19: 739-748, 2013.
13. Wei S, Li Q, Li Z, Wang L, Zhang L and Xu Z: MiR-424-5p promotes proliferation of gastric cancer by targeting Smad3 through TGF-β signaling pathway. Oncotarget 7: 75185-75196, 2016.
14. Zhang Y, Li T, Guo P, Kang J, Wei Q, Jia X, Zhao W, Huai W, Qiu Y, Sun L and Han L: MiR-424-5p reversed epithelial-mesenchymal transition of anchorage-independent HCC cells by directly targeting ICAT and suppressed HCC progression. Sci Rep 4: 6248, 2014.
15. Wang F, Wang J, Yang X, Chen D and Wang L: MiR-424-5p participates in esophageal squamous cell carcinoma invasion and metastasis via SMAD7 pathway mediated EMT. Diagn Pathol 11: 88, 2016.
16. Zhou Y, An Q, Guo RX, Qiao YH, Li LX, Zhang XY and Zhao XL: MiR424-5p functions as an anti-oncogene in cervical cancer cell growth by targeting KDM5B via the Notch signaling pathway. Life Sci 171: 9-15, 2017.
17. Lee JS: Exploring cancer genomic data from the cancer genome atlas project. BMB Rep 49: 607-611, 2016.
18. Livak KJ and Schmittgen TD Analysis of relative gene expression data using real-time quantitative PCR and the 2(-Delta Delta C(T)) method. Methods 25: 402-408, 2001.
19. Wang J, Wang S, Zhou J and Qian Q: MiR-424-5p regulates cell proliferation, migration and invasion by targeting doublecortin-like kinase 1 in basal-like breast cancer. Biomed Pharmacother 102: 147-152, 2018.
20. Li D, Liu K, Li Z, Wang J and Wang X: MiR-19a and miR-424 target TGFBR3 to promote epithelial-to-mesenchymal transition and migration of tongue squamous cell carcinoma cells. Cell Adh Migr 12: 236-246, 2018.
21. Li Q, Qiu XM, Li QH, Wang XY, Li L, Xu M, Dong M and Xiao YB: MicroRNA-424 may function as a tumor suppressor in endometrial carcinoma cells by targeting E2F7. Oncol Rep 33: 2354-2360, 2015.
22. Xu J, Li Y, Wang F, Wang X, Cheng B, Ye F, Xie X, Zhou C and Lu W: Suppressed miR-424 expression via upregulation of target gene Chk1 contributes to the progression of cervical cancer. Oncogene 32: 976-987, 2013.
23. Zhang M, Zeng J, Zhao Z and Liu Z: Loss of MiR-424-3p, not miR-424-5p, confers chemoresistance through targeting YAP1 in non-small cell lung cancer. Mol Carcinog 56: 821-832, 2017.
24. Hershkovitz-Rokah O, Modai S, Pasmanik-Chor M, Toren A, Shomron N, Raanani P, Shpilberg O and Granot G: Restoration of miR-424 suppresses BCR-ABL activity and sensitizes CML cells to imatinib treatment. Cancer Lett 360: 245-256, 2015.
25. Lu M, Kong X, Wang H, Huang G, Ye C and He Z: A novel microRNAs expression signature for hepatocellular carcinoma diagnosis and prognosis. Oncotarget 8: 8775-8784, 2017.
26. Wu CT, Lin WY, Chang YH, Lin PY, Chen WC and Chen MF: DNMT1-dependent suppression of microRNA424 regulates tumor progression in human bladder cancer. Oncotarget 6: 24119-24131, 2015.
27. Yang H, Zheng W, Shuai X, Chang RM, Yu L, Fang F and Yang LY: MicroRNA-424 inhibits Akt3/E2F3 axis and tumor growth in hepatocellular carcinoma. Oncotarget 6: 27736-27750, 2015.
28. Yu L, Ding GF, He C, Sun L, Jiang Y and Zhu L: MicroRNA-424 is down-regulated in hepatocellular carcinoma and suppresses cell migration and invasion through c-Myb. PLoS One 9: e91661, 2014.
29. Wang X, Li Q, Jin H, Zou H, Xia W, Dai N, Dai XY, Wang D, Xu CX and Qing Y: MiR-424 acts as a tumor radiosensitizer by targeting aprataxin in cervical cancer. Oncotarget 7: 77508-77515, 2016.
30. Bartel DP: MicroRNAs: Target recognition and regulatory functions. Cell 136: 215-233, 2009.
31. Kent OA, Fox-Talbot K and Halushka MK: RREB1 repressed miR-143/145 modulates KRAS signaling through downregulation of multiple targets. Oncogene 32: 2576-2585, 2013.
32. Resende TP, Marshall Lund L, Rossow S and Vannucci FA: Next generation sequencing coupled with in situ hybridization: A novel diagnostic platform to investigate swine emerging pathogens and new variants of endemic viruses. Front Vet Sci 6: 403, 2019.